INFORMATION TO USERS

This reproduction was made from a copy of a document sent to us for microfilming. While the most advanced technology has been used to photograph and reproduce this document, the quality of the reproduction is heavily dependent upon the quality of the material submitted.

The following explanation of techniques is provided to help clarify markings or notations which may appear on this reproduction.

1. The sign or "target" for pages apparently lacking from the document photographed is "Missing Page(s)". If it was possible to obtain the missing page(s) or section, they are spliced into the film along with adjacent pages. This may have necessitated cutting through an image and duplicating adjacent pages to assure complete continuity.

2. When an image on the film is obliterated with a round black mark, it is an indication of either blurred copy because of movement during exposure, duplicate copy, or copyrighted materials that should not have been filmed. For blurred pages, a good image of the page can be found in the adjacent frame. If copyrighted materials were deleted, a target note will appear listing the pages in the adjacent frame.

3. When a map, drawing or chart, etc., is part of the material being photographed, a definite method of "sectioning" the material has been followed. It is customary to begin filming at the upper left hand corner of a large sheet and to continue from left to right in equal sections with small overlaps. If necessary, sectioning is continued again—beginning below the first row and continuing on until complete.

4. For illustrations that cannot be satisfactorily reproduced by xerographic means, photographic prints can be purchased at additional cost and inserted into your xerographic copy. These prints are available upon request from the Dissertations Customer Services Department.

5. Some pages in any document may have indistinct print. In all cases the best available copy has been filmed.

University Microfilms International
300 N. Zeeb Road
Ann Arbor, MI 48106

MALCOMSON, MARK ERNIE

AN EVALUATION OF STERIC FIELD FLOW FRACTIONATION FOR PARTICLE SIZE ANALYSIS

THE UNIVERSITY OF ARIZONA M.S. 1984

AN EVALUATION OF
STERIC FIELD FLOW FRACTIONATION
FOR PARTICLE SIZE ANALYSIS

by

Mark Ernie Malcomson

A Thesis Submitted to the Faculty of the

DEPARTMENT OF CHEMISTRY

In Partial Fulfillment of the Requirements
For the Degree of

MASTER OF SCIENCE

In the Graduate College

THE UNIVERSITY OF ARIZONA

1 9 8 4

STATEMENT BY AUTHOR

This thesis has been submitted in partial fulfillment of requirements for an advanced degree at The University of Arizona and is deposited in the University Library to be made available to borrowers under rules of the Library.

Brief quotations from this thesis are allowable without special permission, provided that accurate acknowledgement of source is made. Requests for permission for extended quotation from or reproduction of this manuscript in whole or in part may be granted by the head of the major department or the Dean of the Graduate College when in his/her judgement the proposed use of the material is in the interests of scholarship. In all other instances, however, permission must be obtained from the author.

SIGNED: Mark Malcomson

APPROVAL BY THESIS DIRECTOR

This thesis has been approved on the date shown below:

M F Burke

M. F. BURKE
Associate Professor of Chemistry

10-15-84

Date

TABLE OF CONTENTS

LIST OF TABLES

LIST OF ILLUSTRATIONS

ABSTRACT

Steric Field Flow Fractionation (SFFF) is a technique for the fractionation and size analysis of particles with diameters greater than 0.1μm. Particle separation according to size occurs in a thin channel through which a solvent flows with a laminar solvent velocity distribution.

The details of the construction of a SFFF channel are described. The mechanism of particle separation was investigated by observing the effects of certain experimental parameters on particle retention. These parameters were particle size, channel thickness and solvent density, viscosity and flow rate.

It was found that particle retention was determined not only by particle size, but also certain hydrodynamic forces as well. A model of the forces acting on a particle is used to interpret the results.

CHAPTER 1

INTRODUCTION

Field flow fractionation (FFF) refers to a class of techniques used for the analytical scale separation and characterization of macromolecular and particulate species. FFF is similar to liquid chromatography in that the separation results from the differential migration rates of the sample components through a fixed distance within a liquid carrier. Retention, however, is controlled by an externally applied field rather than by partitioning or adsorption into a stationary phase. The retention behavior in FFF is related to certain physical properties of the analyte species such as size, molecular weight, diffusivity or electrical charge. One can, theoretically, use retention data to characterize the sample components with respect to these properties while performing the separation.

The ability to characterize a sample from retention data can be illustrated by considering the separation process (Figure 1). The separation occurs in a ribbon-like channel through which a solvent flows with a laminar velocity distribution. The size of the channel is typically on the order of 1 cm wide and 100-300 μm thick, with lengths, ranging from 20 to 200 cm. A force or gradient field is applied across the thickness of the channel, perpendicular to the direction of solvent flow. The field can be anything that will interact with the sample

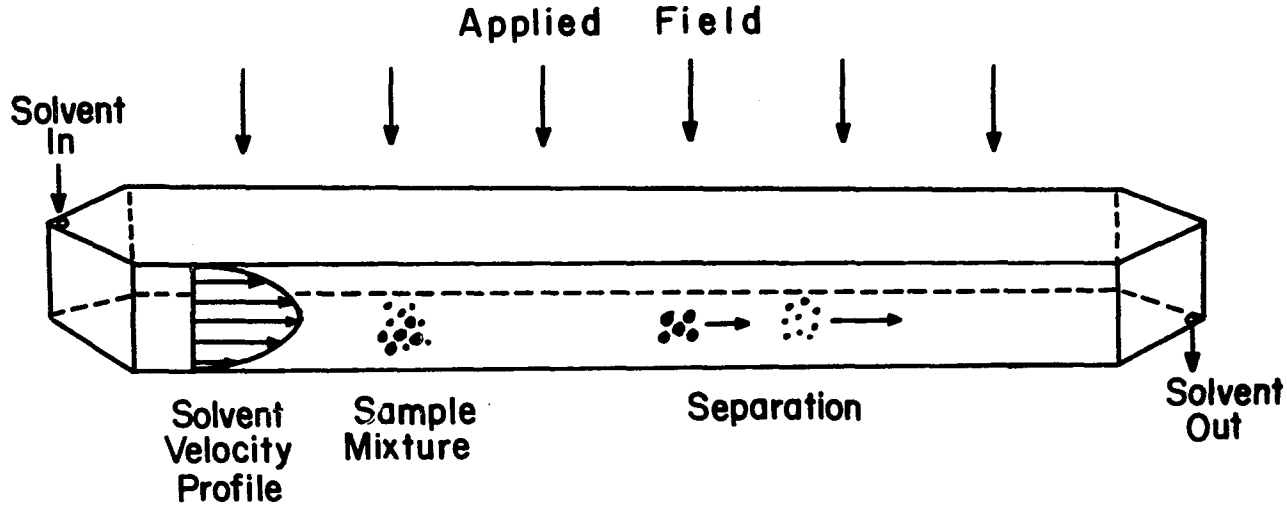

Figure 1. The separation process in FFF.

and induce a motion in the direction of the field. Centrifugal and electrical fields and thermal gradients are examples. This applied field will compress the distribution of components into an area near one channel wall. The degree of compression for each component is determined by an equilibrium between the field-induced motion toward the channel wall and expansion away from the wall by diffusion or brownian motion. Since each component will have a characteristic diffusivity and strength of field interaction, each component will be contained within a layer with a characteristic thickness. This layer thickness will determine what portion of the parabolic velocity profile of the solvent flow impacts on the component and, hence, the component's average velocity through the channel. Generally, large components will form thinner layers and move more slowly through the channel than the small components which can diffuse into faster solvent flowstreams. With the simple channel geometry used, the solvent velocity distribution is well-defined mathematically. The component's elution time can thereby be related to the layer thickness which, in turn, is directly related to the physical properties of the component.

The relationship between layer thickness and component characteristics can be described in the following manner. The concentration distribution of the component in equilibrium with the field is exponential as given by[1]

$$c = c_o e^{-x/\ell} \qquad (1)$$

where c is the concentration of the component at distance x from the channel wall, c_o is the concentration at the wall, and ℓ is given by

$$\ell = {}^{D}/_{U} \tag{2}$$

where D is the component's diffusion coefficient and U is the average field-induced velocity. A more useful measure of layer thickness is the dimensionless parameter λ, given by [1]

$$\lambda = {}^{\ell}/_{w} = {}^{D}/_{Uw} \tag{3}$$

where w is the thickness of the channel. Integration of the concentration distribution across the solvent velocity distribution for laminar flow between infinite parallel plates yields [1]

$$R = {}^{V_o}/_{V_r} = 6\lambda[\coth({}^{1}/_{2\lambda}) - 2\lambda] \tag{4}$$

where R, the retention ratio, is defined as the ratio of channel void volume, V_o, to component retention volume, V_R. For R values less than 0.5, Equation (4) simplifies to [1]

$${}^{V_R}/_{V_o} = {}^{1}/_{6\lambda} + {}^{1}/_{3} \tag{5}$$

These equations relate retention data to various physical properties of the sample components (Table 1).

One of the inherent advantages of FFF is the external control of retention. By varying the field strength, one can go from a condition of nearly complete retention to zero retention. This enables one to analyze a complex mixture containing a broad range of components

Table 1. Solute Parameters in FFF

Technique	Solute parameters controlling retention
Sedimentation FFF	M, $\overline{V}_s$, S, D
Flow FFF	D, d
Electrical FFF	μ, D
Thermal FFF	D_T, α

M = molecular weight

$\overline{V}_s$ = partial molar volume of solute

S = sedimentation coefficient

D = solute-solvent diffusion coefficient

d = stoke's diameter

μ = electrophoretic mobility

D_T = thermal diffusion coefficient

α = thermal diffusion factor

in a single run. This high peak capacity and positive control of retention gives the analyst great versatility in determining the speed and resolution of an analysis. Furthermore, since FFF is an elution technique, detection and fraction collection can be easily and reproducibly accomplished. Finally, the FFF channel presents a minimal surface area to the sample thus reducing the chances of reactive or adsorptive interactions.

The disadvantages of FFF stem primarily from specific technical aspects of the various subtechniques. In thermal FFF,[2,3] a constant thermal gradient must be maintained along the full length of the channel. Also, in order to establish a large enough gradient for good resolution, it may be necessary to operate the channel under pressure to avoid boiling the solvent. This places a greater demand on the channel seals. In electrical FFF,[4,5] problems may be caused by ohmic heating and nonuniformity of the electric field. In flow FFF,[6,7] a semi-permeable membrane is used for the channel walls to allow for the lateral solvent flow. This membrane must be mechanically rigid and highly and uniformly permeable to the solvent yet impermeable and nonsorptive to the solutes. In sedimentation FFF,[3,7,10] where the field is generated by a centrifuge, the field strength is limited by the mechanical stability of the seals through which the solvent flows into and out from the centrifuge. However, this is not a severe limitation and sedimentation FFF is likely to find wide-spread application in the near future.[11]

One subtechnique, steric FFF,[12] is an interesting variation of the normal FFF method. Steric FFF is applicable to particles with diameters of >0.1μm and can be used with any field which will force the particles into contact with one of the channel walls. Such forces would include a centrifugal force or, for particles>1μm, simply the earth's gravitational force. Once in contact with the channel wall, the size of the particles will determine what portion of the solvent velocity gradient impacts on the particles and hence their velocity

through the channel. Large particles will extend into faster flow-streams than small particles, giving a large to small particle elution order, which is the inverse of normal FFF.

Unlike the other FFF techniques, the design and construction of a gravitational steric FFF system requires no special technical developments. Implementation of such a system provides a straightforward means of investigating the FFF method of separation. Furthermore, as an elution technique, the potential speed, simplicity and sensitivity offered by steric FFF as a particle sizing tool would provide distinct advantages over present techniques applicable to this particle size range: sieve analysis, microscopy, sedimentation and light transmission or scattering are either slower and more tedious or require complex, expensive instrumentation. For these reasons, an evaluation of steric FFF was warranted.

The goal of this investigation was to evaluate the potential usefulness of steric FFF as a particle size analysis technique. The approach was to measure the rate of movement of various particles through the channel and to determine what effect changes in the basic experimental parameters had on this rate. These parameters included the velocity, density and viscosity of the liquid carrier, and channel thickness.

CHAPTER 2

EXPERIMENTAL METHODS AND MATERIALS

The instrumentation in a steric FFF system is basically the same as that found in a liquid chromatographic system. The fractionation channel is supported by a solvent pump, sample injector, flow-through detector, and flow-measuring device. The construction of the channel, and supporting instrumentation and the experimental procedures used will be described in this chapter.

Channel Construction

The design of the steric FFF channel used (Figure 2) was modeled after one reported by Giddings[1]. The spacers were formed by cutting 1.0 x 111 cm channels out of the center of Mylar sheets, 8 x 122 cm in size, with thicknesses of 127, 173 and 254 μm. A channel was sandwiched between two pieces of float plate glass, 8 x 122 cm in size, 1.3 cm (0.5 in) thick. This sandwich was clamped together between a 0.95 cm (3/8 in) aluminum and a 2.5 cm (1 in) plexiglass clamping bars, both 13 x 122 cm in size. The plexiglass was mounted on the upper surface so that the condition of the channel could be visually monitored. Two 4.0 x 122 cm strips of clear vinyl were placed between the clamping bars and glass plates to serve as cushions and to help maintain pressure on the center of the glass plates rather

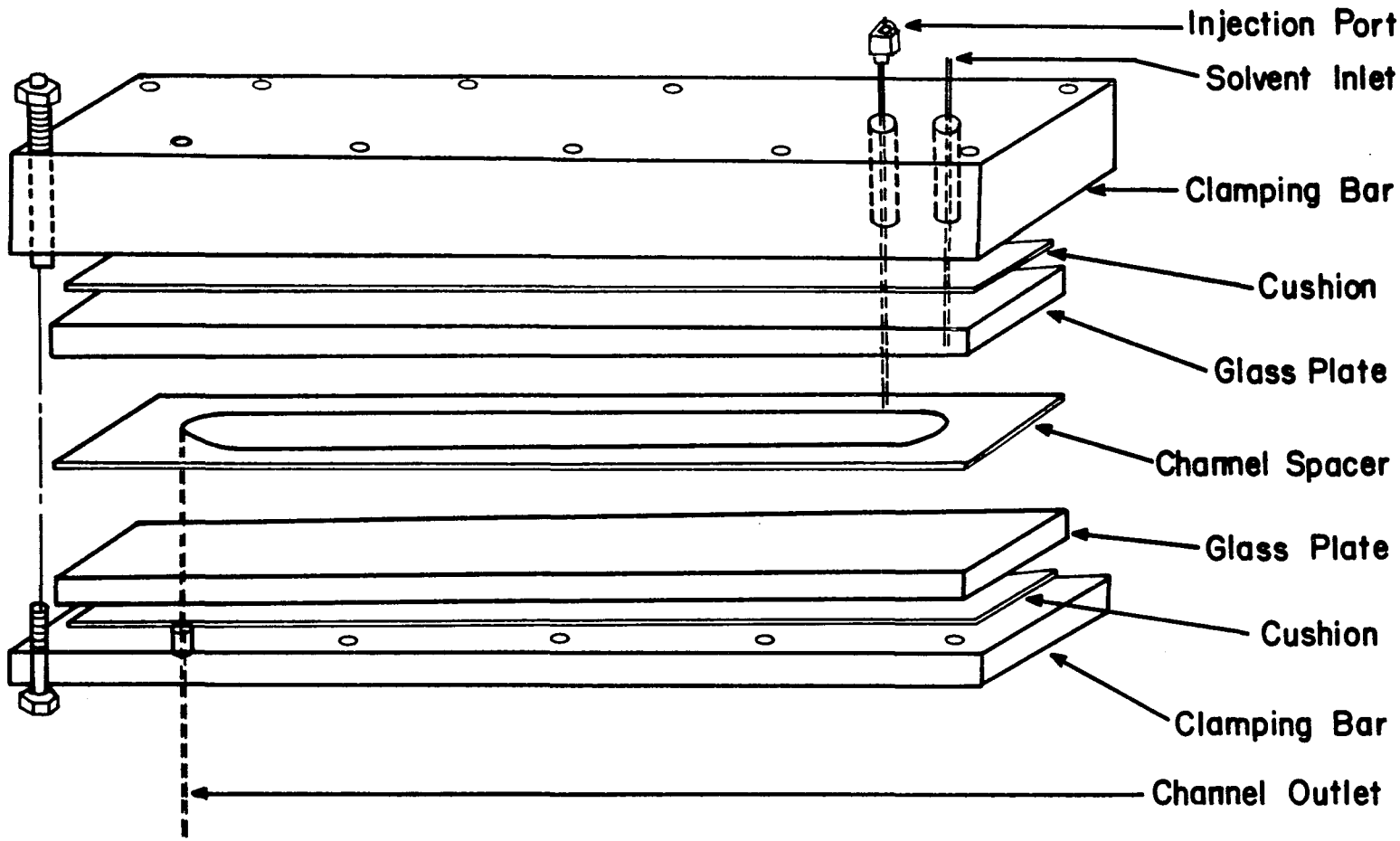

Figure 2. Schematic drawing of steric FFF channel.

than the outer edges. Clamping pressure was maintained by bolts placed every four inches along each side of the channel, torqued to 8 ft-lbs. Solvent entered and exited the channel through 1/16" stainless steel tubing expoxied into holes drilled through the glass plates. The channel was positioned horizontally so that the earth's gravity would provide the necessary field. The tubing was configured so that solvent entered through the top plate and exited downward through the bottom plate to avoid transporting particles against gravity.

The samples were injected through a septum device made from a 1/4 to 1/16 inch Swagelok(R) reducing union. The septum was held in place with a nut in the 1/4 inch end of the union. The other end of the union was fastened to a piece of 1/16 inch stainless steel tubing which was epoxied into a hole through the upper glass plate. The length of the tubing was such that, upon insertion, a 2-inch needle would extend to just above the channel surface. This injector was located 2 cm downstream from the solvent entrance of the channel.

Support Instrumentation and Materials

The requirements on the solvent delivery pump were simply that it deliver precise, relatively pulseless flow in the range of 1.0 to 8.0 ml/min. Two commercial liquid chromatographic solvent pumps were used: an Altex Model 110A Solvent Metering Pump (Berkeley, CA) and a Spectra Physics Model SP3500 Liquid Chromatograph (Santa Clara, CA). Both pumps performed satisfactorily. To help dampen pump pulses, a

---

(R) Crawford Fitting Co.

flow restrictor, composed of 15 cm of 1/8 inch tubing filled with 40 μm glass beads, was placed between the pump and channel.

For detecting the elution of the particles, a Schoeffel Model 770 Variable Wavelength Spectrophotometric Detector (Klane Scientific, Tustin, CA) was used. The heat exchanger was removed and the flow direction through the cell was reversed for downward flow to reduce peak broadening and particle accumulation in the flow cell. No significant change in response wavelength was observed. Detector output was displayed on a Linear (Linear Instruments Corp., Reno, Nevada) chart recorder.

Flow rate was measured by directing the flow upward into a 50 ml buret and timing the rate of rise. A length of 3/8 inch Tygon tubing formed into a U between the detector and buret trapped the particles and prevented clogging of the buret.

All solvents used, except water, were analytical reagent grade and used without further purification. Water was house-distilled water, redistilled from basic permanganate. All solvents were filtered through a 0.45 μm membrane and vacuum degassed immediately prior to use.

Most of the data was taken using solid, spherical glass beads with diameters of 8.0 μm (22% RSD) and 20.0 μm (8.0% RSD) (Duke Scientific, Palo Alto, CA). Also used were 5 and 10 μm Lichrosorb, an irregular porous silica, and 5 and 10 μm Spherosorb (Rainin Instrument Co., Wobum, Mass.), a spherical porous silica. All particles were

dispersed in the carrier solvent with ultrasonication. Porous particles were ultrasonicated under a vacuum to dispel air from the pores.

Experimental Methods

Samples were redispersed ultrasonically immediately prior to injection. A 50 µl syringe was used to inject 20 - 40 µl samples into the channel for dispersions containing 10 - 20 mg particles per ml of solvent.

Solvent flow was stopped before injection, then reinstated after allowing time for the particles to settle to the lower channel wall. This relaxation time was approximately five to ten minutes depending on particle size, solvent density and viscosity.

The retention time of given peak was measured at the midpoint of the peak at a line drawn through the half-height of the peak parallel to the baseline. This was used instead of the peak maximum because the peak maximum was frequently jagged and irregular. Retention times were converted to average particle velocities by dividing the channel length by retention time. Average solvent velocities were calculated by dividing the measured flow rate by channel thickness x channel width. A sample fractogram is shown in Figure 3.

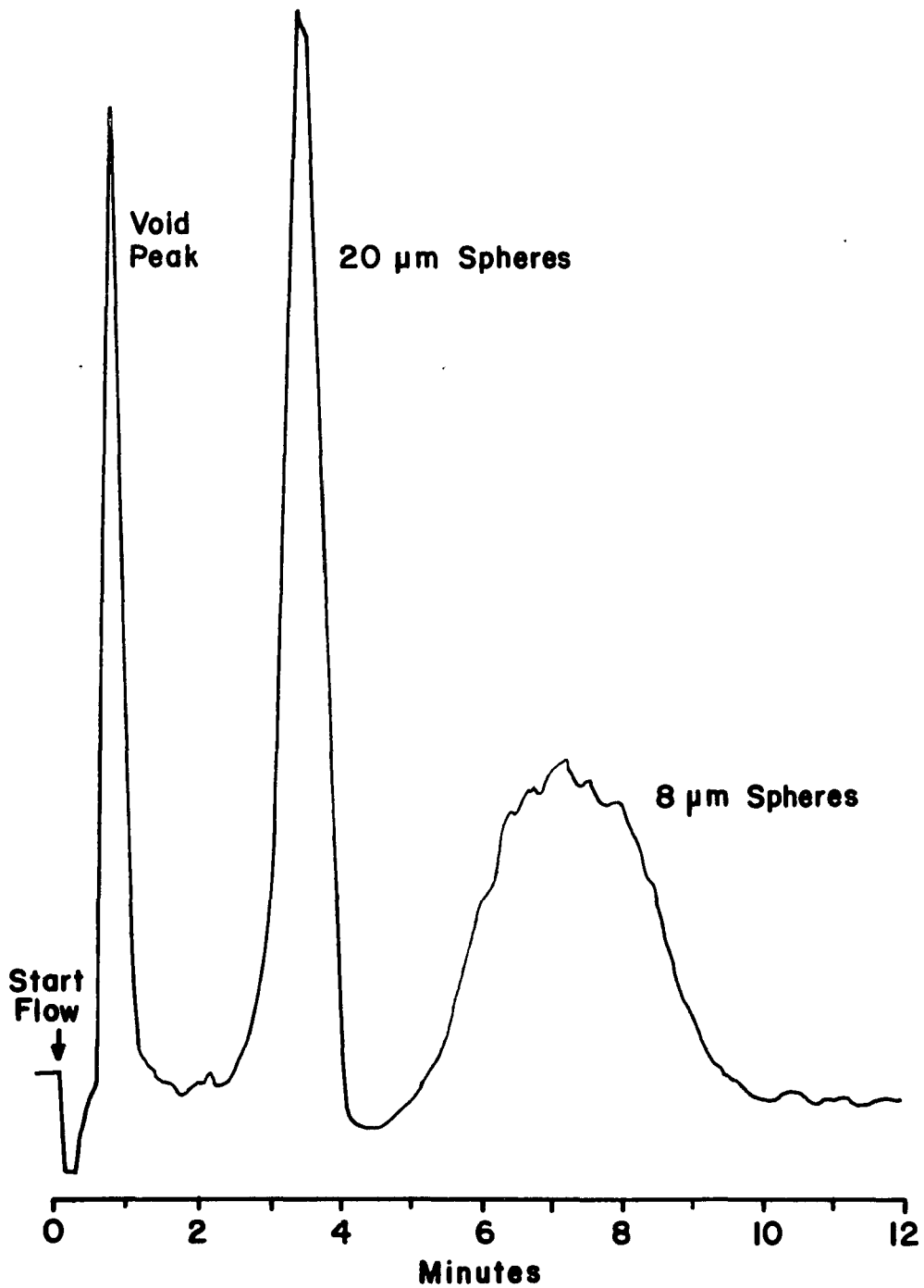

Figure 3. Separation of 20 µm (±8% RSD) and 8 µm (±20% RSD) in 173µm channel, 10% (V/V) methanol in water, at 3.6 ml/min.

CHAPTER 3

PARTICLE RETENTION IN STERIC FFF

Theoretical Considerations

The separation capability of FFF is based on the parabolic distribution of fluid velocity for laminar flow between parallel plates. This velocity distribution is given by[13]

$$V = \frac{\Delta P}{2 \mu l} X (h - X) \qquad (7)$$

where V is the fluid velocity at distance X from one channel wall, Δp is the pressure drop across length l, μ is the fluid viscosity, and h is the distance between the channel walls. In FFF, retention of sample components is achieved by compressing the components into the slow moving fluid region near the channel wall with an applied field. In conventional FFF, there is random motion, through diffusion or brownian motion, which opposes the field to produce a layer with a finite thickness in which a component is distributed. Two components will become separated as they flow through the channel if their differences in random motion or strength of field interaction produces layers of different thicknesses. Steric FFF is an extension of FFF to particles larger than $\sim$0.1 μm where the random motion is small compared to the dimensions of the particles. The particles are brought to the channel wall by gravity or a sedimentation field so that the size of

the particles determine what portion of the parabolic fluid velocity distribution impacts on the particles, and hence their velocity through the channel.

Originally it was expected[12] that a spherical particle would move along the wall of the channel with a velocity approximately equal to the velocity of the solvent at the center of the particle. This velocity could be calculated from Equation 7 by setting X equal to the particle radius, or, as a relative value, from

$$V_p/V_s = 6\ a/h\ (1 - a/h) \tag{8}$$

where V_p is the particle velocity, V_s is the average solvent velocity (velocity of an unretained solute), a is the particle radius, and h is the channel thickness. The ratio V_p/V_s is equivalent to R, the retention ratio of FFF,

$$R = V_o/V_R = 6\ a/h(1 - a/h) \tag{9}$$

where V_0 is the channel void volume and V_R is the particle retention volume. For reasonable retention, the particle size should be small compared to the channel thickness ($a \ll h$) so that R can be approximated by

$$R \simeq 6\ a/h \tag{10}$$

This equation provides a measure of particle retention based on the solvent velocity distribution of laminar flow.

However, with the initial experimental results it became apparent that particle retention is influenced by certain hydrodynamic effects which were not observed with the colloidal and macromolecular samples of conventional FFF. The significance of these

effects is shown by Figure 4. The most notable aspect shown here is the increase in R with increasing flow rate.

Departures from theory were also observed by Giddings and co-workers.[14] They attributed low R values to a viscous resistance to particle rotation and suggested that a drag factor, γ, be included in Equation 10

$$R = 6\gamma\, a/w \tag{11}$$

with γ being less than one. They also suggested that the increase in R with flow rate was caused by a solvent velocity dependent lift force which would raise the particles away from the channel wall and into faster solvent flowstreams. This was supported by the observations that for particles with the same size but different densities, the more dense particles were retained longer. Also, increasing the centrifugal field strength increased particle retention.

The origins of such a lift force are not readily apparent, but evidence for the existence of this phenomenon can be found in the literature. Rubinow and Keller,[15] for example, found in a theoretical study that a spinning sphere moving in a viscous fluid would be subject to a force orthoganol to its direction of motion. The magnitude of this force was given by

$$F_L = \P a^3 \rho\Omega \times V_p(1 + O(R)) \tag{12}$$

where a is the particle radius, Ω is its angular momentum, ρ is the fluid density, V_p is the particle's velocity and R is its Reynolds number. In steric FFF, the particles will probably be spinning because of the velocity gradient across the diameter of the particle. Saffman,[16]

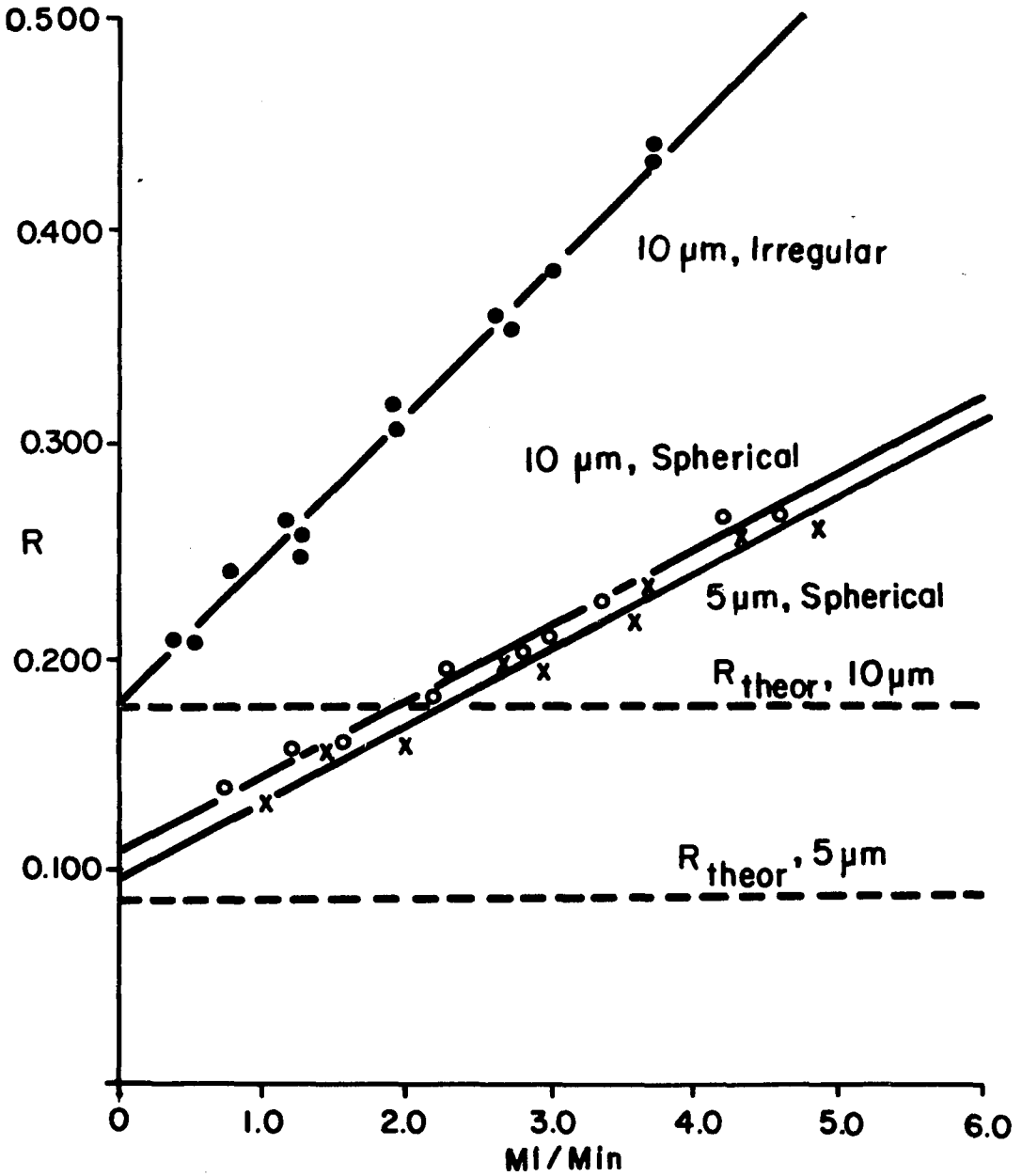

Figure 4. Retention of irregular (Lichrosorb) and spherical (Spherisorb porous silica particles.

in another theoretical study, has shown that a rigid spherical particle in uniform shear flow (linear flow velocity gradient) through a tube of radius h should be subject to a lateral force given by

$$F_L = 164.4\ V_p\ a^2\ (\rho\ \eta)^{1/2}\ (y\ V_s/h^2)^{1/2} \qquad (13)$$

where a and ρ are defined as above, V_p is the velocity of the particle measured relative to the flowstream at the center of the particle, η is the fluid viscosity, V_s is the average fluid velocity and y is the distance of the particle from the tube axis. Segre' and Silberberg[17,18] have experimentally demonstrated the "pinched tubular effect" in which spheres suspended in a neutrally buoyant medium flowing through a tube migrated to an annular region at $\sim$0.6 of the tube radius from the axis. They found that this effect depended on the cube of the particle radius and that the origin of the lateral force was in the inertia of the fluid. None of the above treatments are strictly applicable to steric FFF because of differences in flow geometry, Reynolds number and treatment of the wall effect. The wall effect is especially important in steric FFF because of the proximity of the particles to the wall. Nevertheless, these reports do provide evidence for the existence of a lift force and suggest what parameters are of importance to the magnitude of this force.

An evaluation of the effect of these parameters on particle retention should contribute to a more complete description of the mechanism of particle retention in steric FFF. Towards this end, spherical, solid glass beads were run through channels of different

thicknesses in solvents with different densities and viscosities. To aid in the interpretation of the results of these experiments, a simple model of the forces acting on a particle will be used.

In this model (Figure 5) the downward force, F_g, is the gravitational pull on the particle. This is opposed by the lift force, F_L, which has two components. The first component is a constant force from the buoyancy of the solvent which is proportional to the solvent density. The second component is the hydrodynamic lift force which, as discussed earlier, increases with increasing flow rate. The shear force of the solvent, F_S, which pushes the particles through the channel, is a combination of the viscous drag and dynamic pressure on the particle. The retarding force, F_R, represents any process or interactions which would cause the particle to lag behind the solvent. One source of this lag could be the rotational motion of the particle caused by the solvent velocity gradient across the diameter of the particle. Energy would be expended through both the rotational energy of the particle and viscous drag against particle rotation. Another possible retarding action could result from the resistance of the nearly stagnant layers of solvent adjacent to the channel wall or by frictional resistance between the particle and channel surfaces. The combination of these four forces as a model provides a means for explaining how the various experimental parameters affect particle motion through the channel.

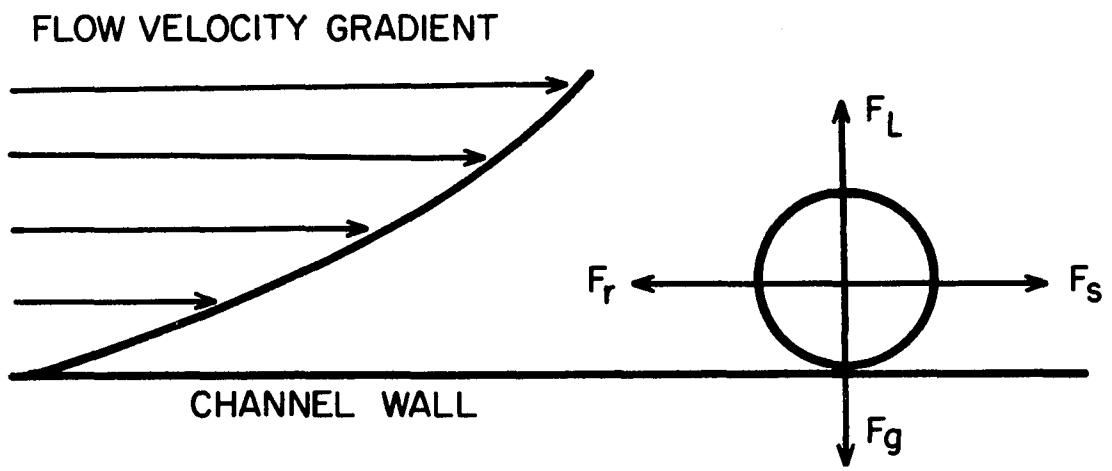

Figure 5. Model of forces acting on a particle in a steric FFF channel.

Results and Discussion

The effect of the various experimental parameters on particle retention is illustrated by graphs of R versus V_S. The variation of particle retention between channels of different thicknesses is shown in Figures 6 and 7. Figure 8 illustrates the effect of solvent viscosity on particle retention. Figure 9 shows the variation in particle retention with changes in solvent density. A discussion of each of these cases will be based on the following considerations.

These graphs show a linear dependence of R on solvent velocity, V_S, and a positive R intercept. Thus, an equation relating particle retention to solvent velocity would have the form

$$R = mV_S + b \tag{14}$$

where m is the slope and b is the intercept of an R versus V_S graph. Considering the forces acting on the particles, this relationship can be interpreted in the following manner. The slope, m, reflects the contribution of the hydrodynamic lift force to R. Since this lift force is solvent velocity dependent, extrapolation to $V_S = 0$ removes this contribution to R. The R value of the intercept represents the minimum relative particle velocity for a given particle and is limited by the size of a particle. In other words, the size of the particle excludes it from the slower moving solvent closer to the channel wall. Based on the laminar solvent velocity distribution, this minimum relative velocity would be given by Equation 9. However, the actual minimum velocity would also be affected by the magnitude of the

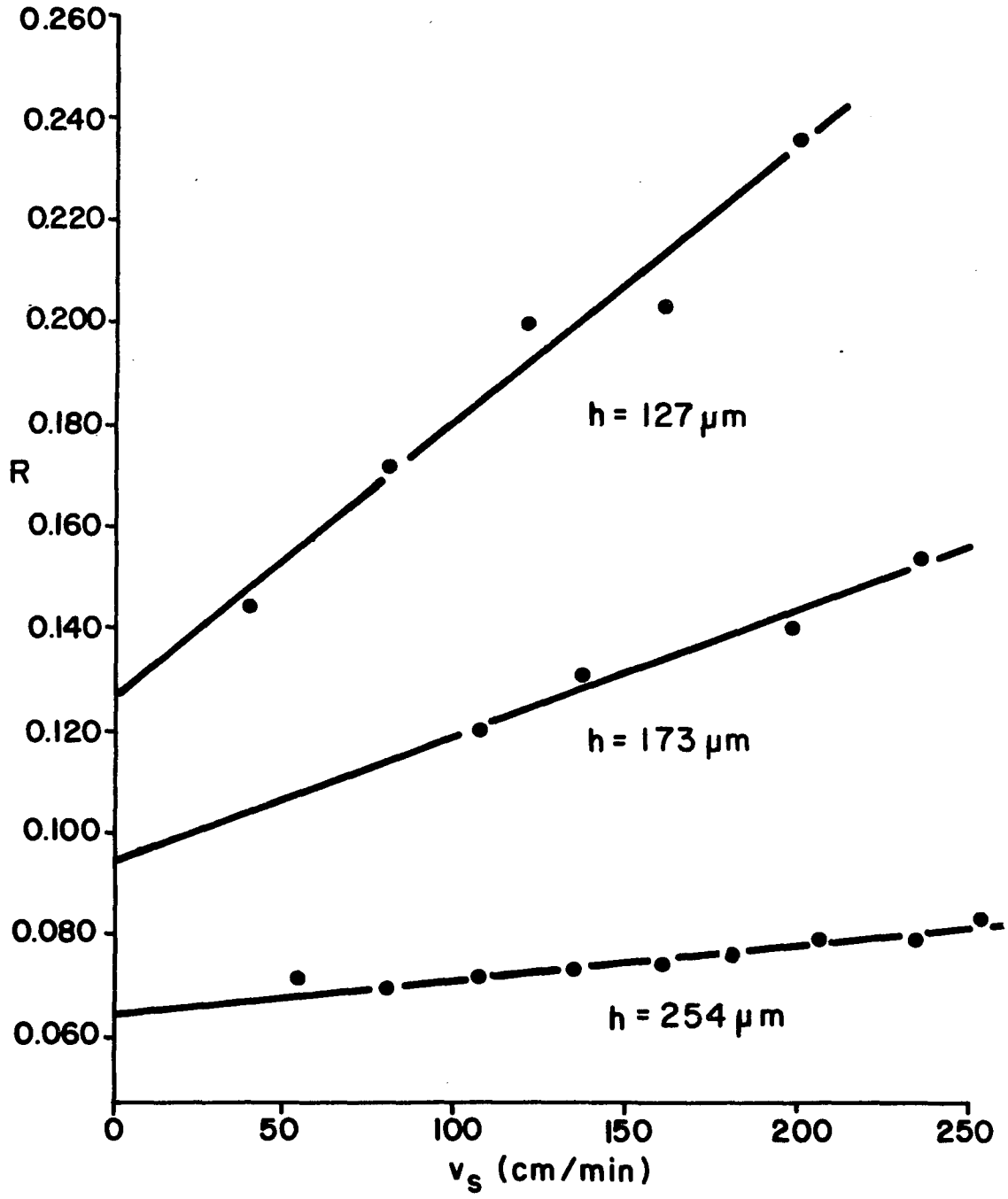

Figure 6. Retention as a function of solvent velocity for 8µm spheres in 10% (V/V) methanol in water.

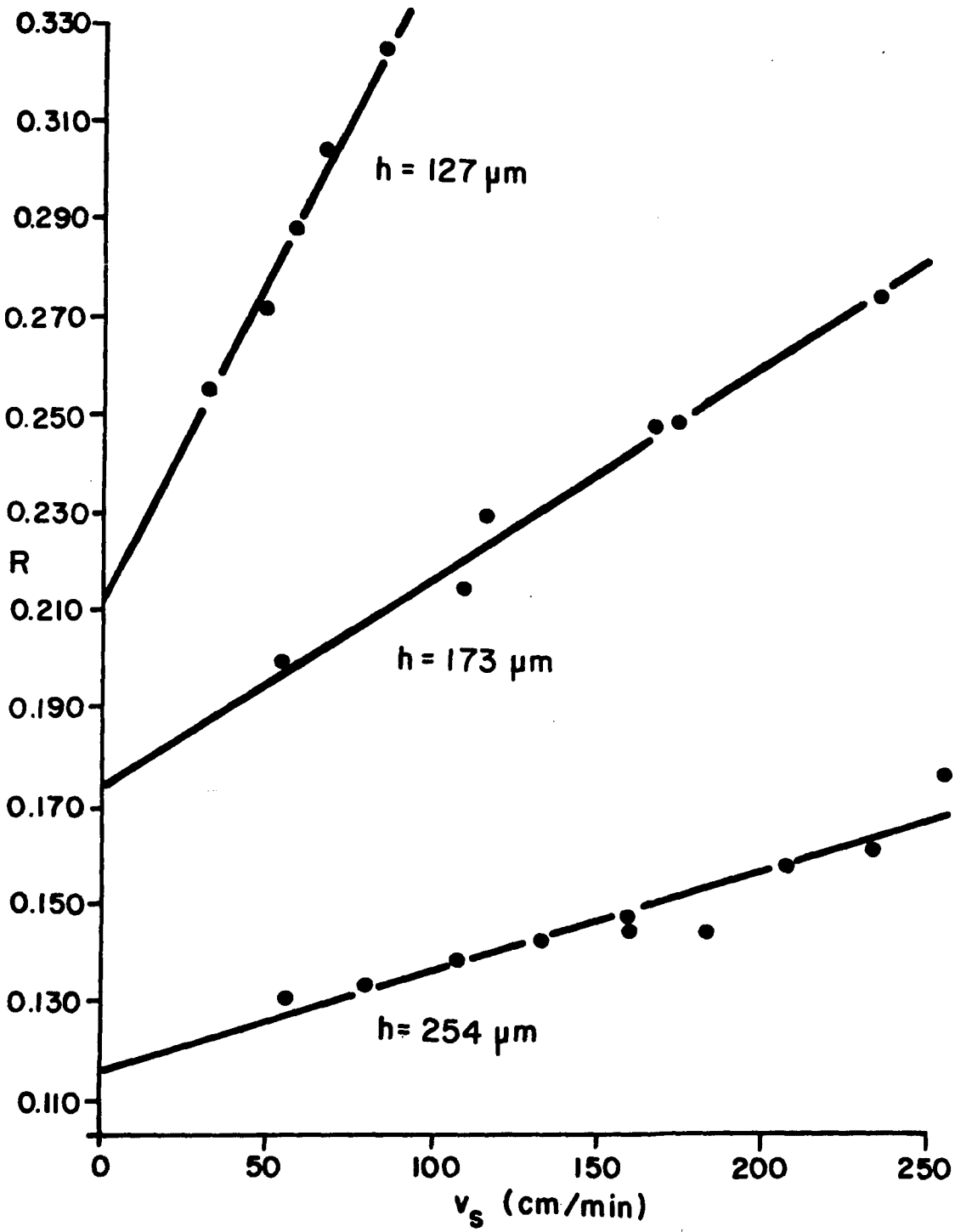

Figure 7. Retention as a function of solvent velocity for 20µm spheres in 10% (V/V) methanol in water.

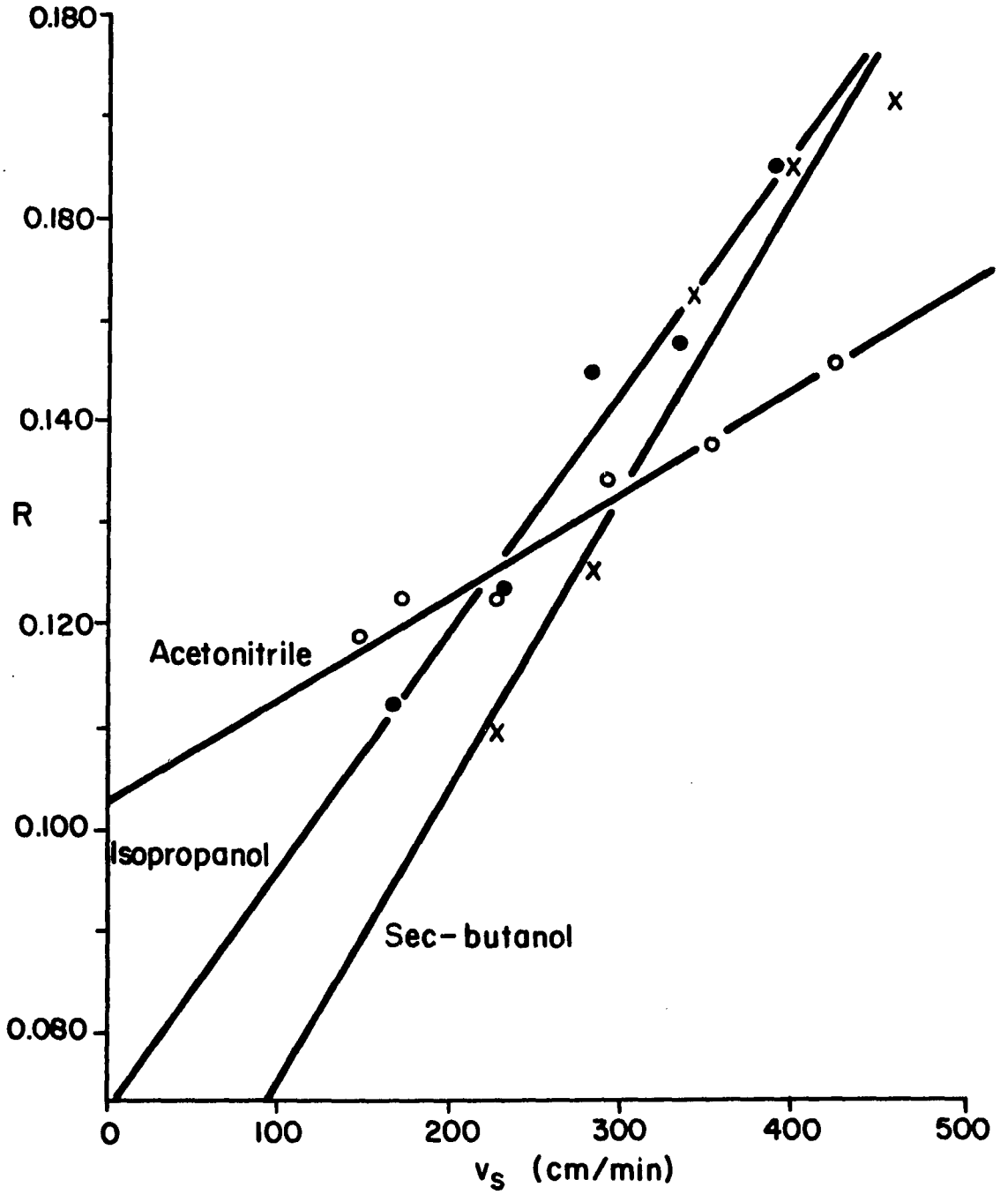

Figure 8. Retention of 8μm diameter spheres in solvents with similar densities.

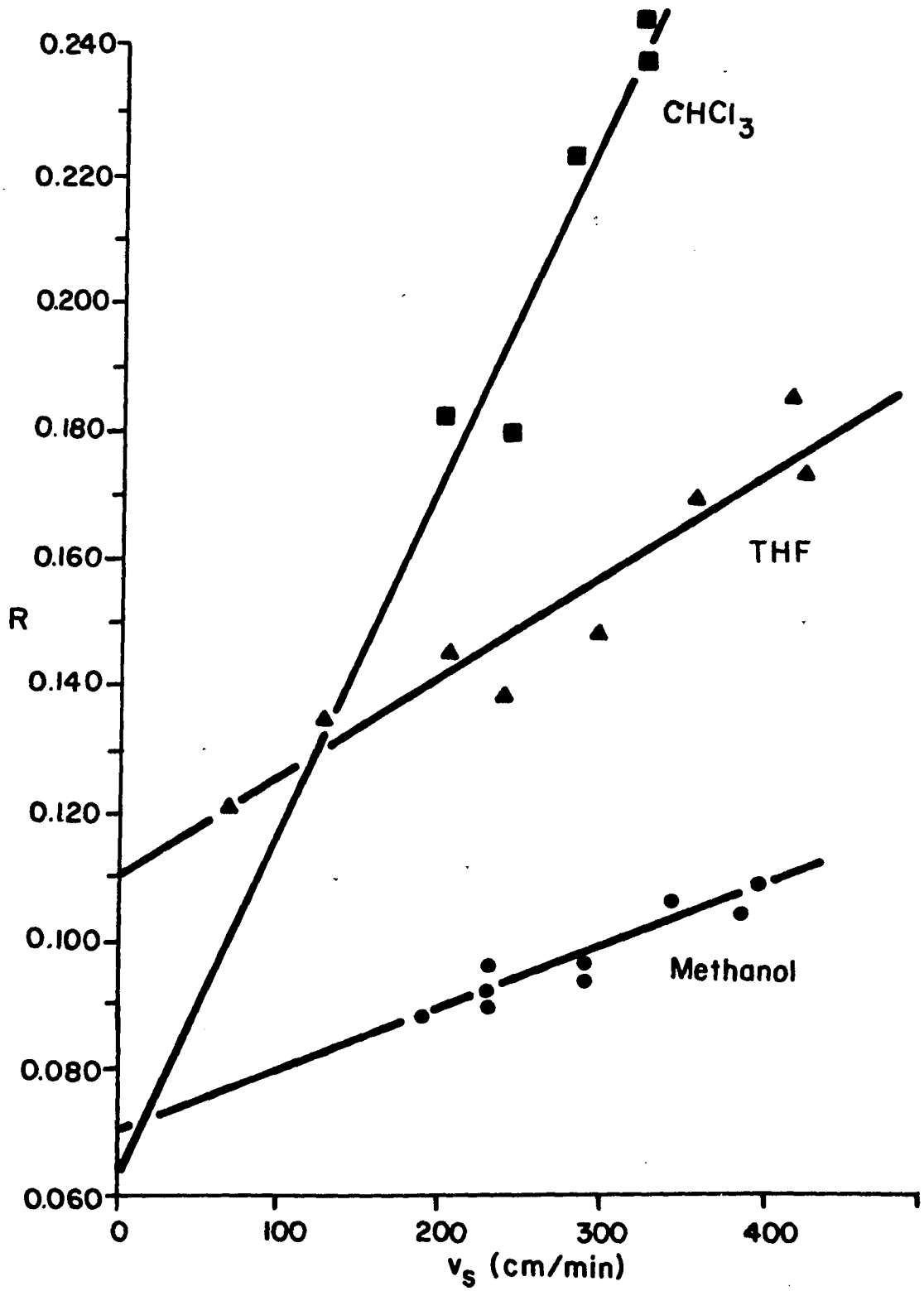

Figure 9. Retention of 8μm diameter spheres in solvents with similar viscosities.

retarding force, F_R. Using the drag factor, γ, to account for the lage of the particle behind the solvent, the following equation is proposed for describing particle retention;

$$R = mV_s + 6\gamma(a/h)(1 - a/h) \quad (15)$$

This description of particle retention is supported by the data taken with channels of different thicknesses. The values in Table 2 were calculated from the data shown in Figures 6 and 7. The slope, intercept and correlation coefficients were calculated by least-squares regression. The $\Delta a/\Delta V_s$ values were obtained by setting the slope ($\Delta R/\Delta V_s$) equal to R in Equation 9 and solving for a. This normalizes the slopes to channel thickness and allows a direct comparison of the slopes as a measure of the lift force. The R intercepts were also expressed in terms of a, the calculated particle radius, by using the same equation. The γ values are the ratios of the calculated radii to the actual particle radii.

The concept that the R intercept is the lower limit of retention and is determined by the size of the particles and the magnitude of F_R is supported by the channel to channel consistency of the calculated radii (a_{int}) and γ values for each particle size. This follows from the fact that the retarding force, F_R, is determined by particle rotation or surface interactions, and would be expected to be independent of channel thickness, as is shown by the consistency of the values.

Table 2. Effects of Channel Thickness on Particle Retention

Particle radius (μm)	4	4	4	10	10	10
Channel thickness (μm)	127	173	254	127	173	254
Slope ($X10^4$)	5.42	2.44	0.647	13.5	4.38	2.07
Intercept	0.127	0.0949	0.0646	0.213	0.175	0.117
Correlation Coefficient	0.78	0.98	0.95	0.99	0.99	0.92
a from intercept	2.75	2.78	2.76	4.68	5.20	5.05
$\Delta a/\Delta V_s$ from slope ($X10^3$)	11.4	7.0	2.7	28.5	12.6	8.8
γ	0.688	0.695	0.690	0.468	0.520	0.505

A comparison of the γ values obtained for the two particle sizes indicates that F_R is greater for the larger particle. This is consistent with the force model since one would expect F_R to be greater for a particle with greater mass and surface area.

The effect of channel thickness of F_L is shown by comparing the $\Delta a/\Delta V_s$ values for each of the particles. These values show an increase in F_L with decreasing channel thickness, which is consistent with the earlier discussion of the hydrodynamic lift force. It was also expected from this discussion that F_L would increase with increasing particle size. This was observed and is shown by comparing the $\Delta a/\Delta V_s$ values for the two particle sizes. This particle size dependence also explains why the effect of F_L on R has not been significant with the much smaller samples of conventional FFF.

The effect of solvent viscosity on particle retention is shown in Figure 8 and Table 3. The three solvents had a wide range of viscosities but approximately the same density. The intercept and

values indicate that F_R increases with increasing viscosity, which was expected from the force model. Although this would tend to increase particle retention, increasing solvent viscosity also decreased retention by contributing to F_L, as shown by the slope values. The exact magnitude of this contribution is somewhat obscured since increasing viscosity will also increase the resistance to particle motion in the direction of F_L.

Table 3. Effects of Solvent Properties on Particle Retention

Solvent	μ(cp @ 15°C)	ρ(g/cm^3 @ 15°C)	a_{calc}(μm)	γ	$\Delta a/\Delta V_s$
Acetonitrile	0.375	0.787	2.9	0.725	3.5
Isopropanol	2.86	0.785	2.1	0.525	6.9
Sec-Butanol	4.21	0.804	1.4	0.350	8.0
Methanol	0.623	0.792	2.0	0.500	2.7
Tetrahydrofuran	0.60	0.889	2.4	0.600	7.2
Chloroform	0.596	1.48	1.9	0.475	16

To study the effects of density, solvents were selected which had similar viscosities but different densities. The results are shown in Figure 9. The results here are somewhat inconclusive because chloroform and methanol both produced broad, irregular peaks at low

flow rates. This may be caused by ineffective lubrication or wetting of the particles, as will be discussed later. Comparing particle retention in chloroform and methanol, solvent density does not appear to have a significant effect on F_R as shown by the intercepts. It does, however, appear to contribute to F_L. The increase in F_L with density is greater than would be expected from increased buoyancy alone. For these particles (density = 2.45 g/cm^3), going from methanol to chloraform would increase the buoyant force by a factor of 1.7. The slope, however, increased by a factor of 5.9, indicating an increase in the magnitude of the hydrodynamic lift force.

The possibility of a surface or solvation effect was investigated with solvent mixtures of methanol and tetrahydrofuran (THF). The depressed retention and broader peaks obtained with methanol were evident in mixtures containing up to 90% THF (Figures 10 and 11). This "methanol-like" behavior even at relatively low concentrations of methanol indicates a surface effect as opposed to an effect resulting from the bulk properties of the mixtures.

This raises the question of how a surface interaction occurs for a particle that's been lifted away from the channel surface. Up until this point, for the sake of clarity, particle retention has been discussed in terms of a single particle moving smoothly through the channel. It is more realistic to assume that, at the micron level, there are irregularities in the channel surface, nonuniformities in the channel thickness and flow distribution, and distortions in the shape of the particles, all of which would contribute to oscillations

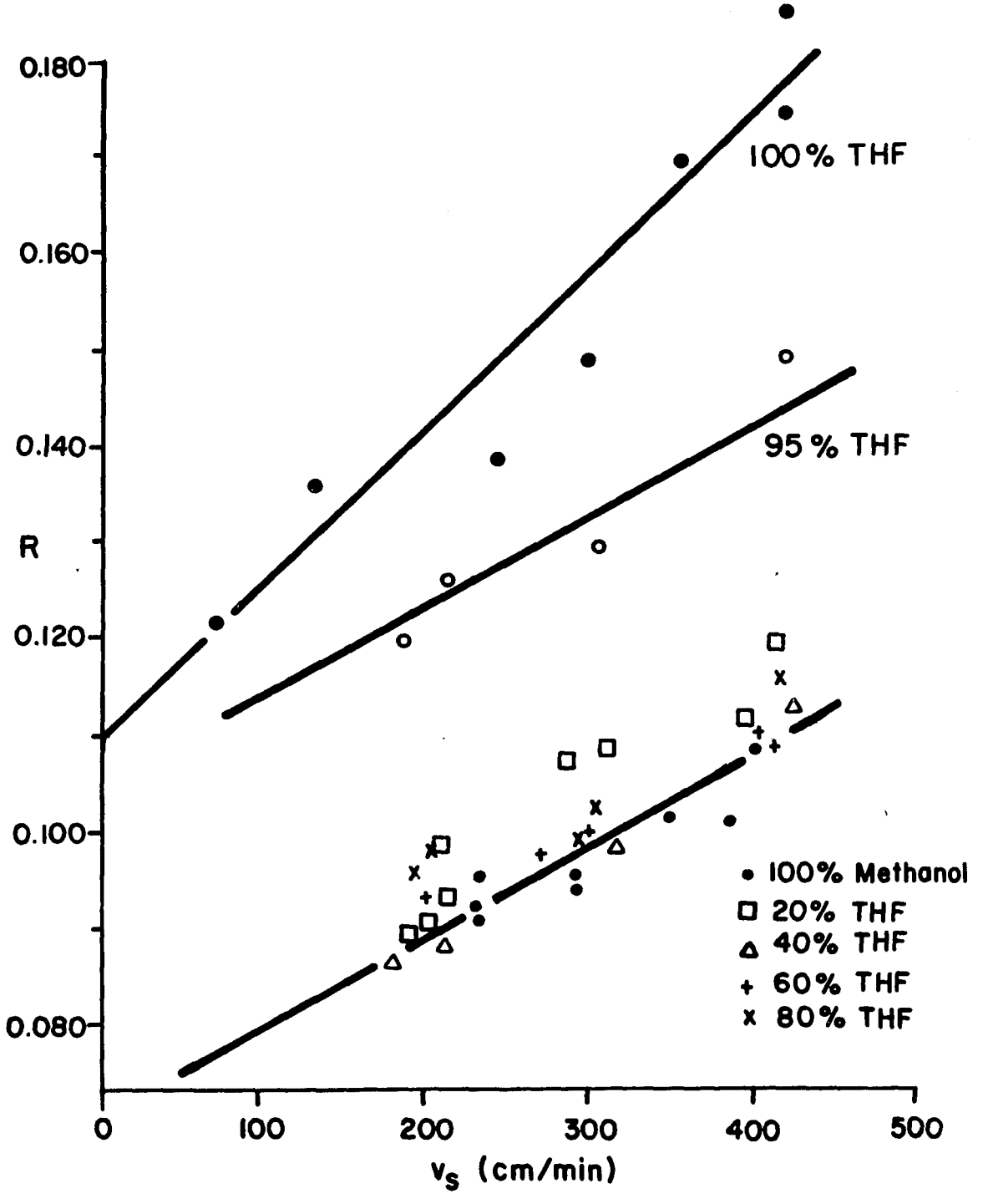

Figure 10. Retention of 8μm diameter spheres in tetrahydrofuran methanol solutions.

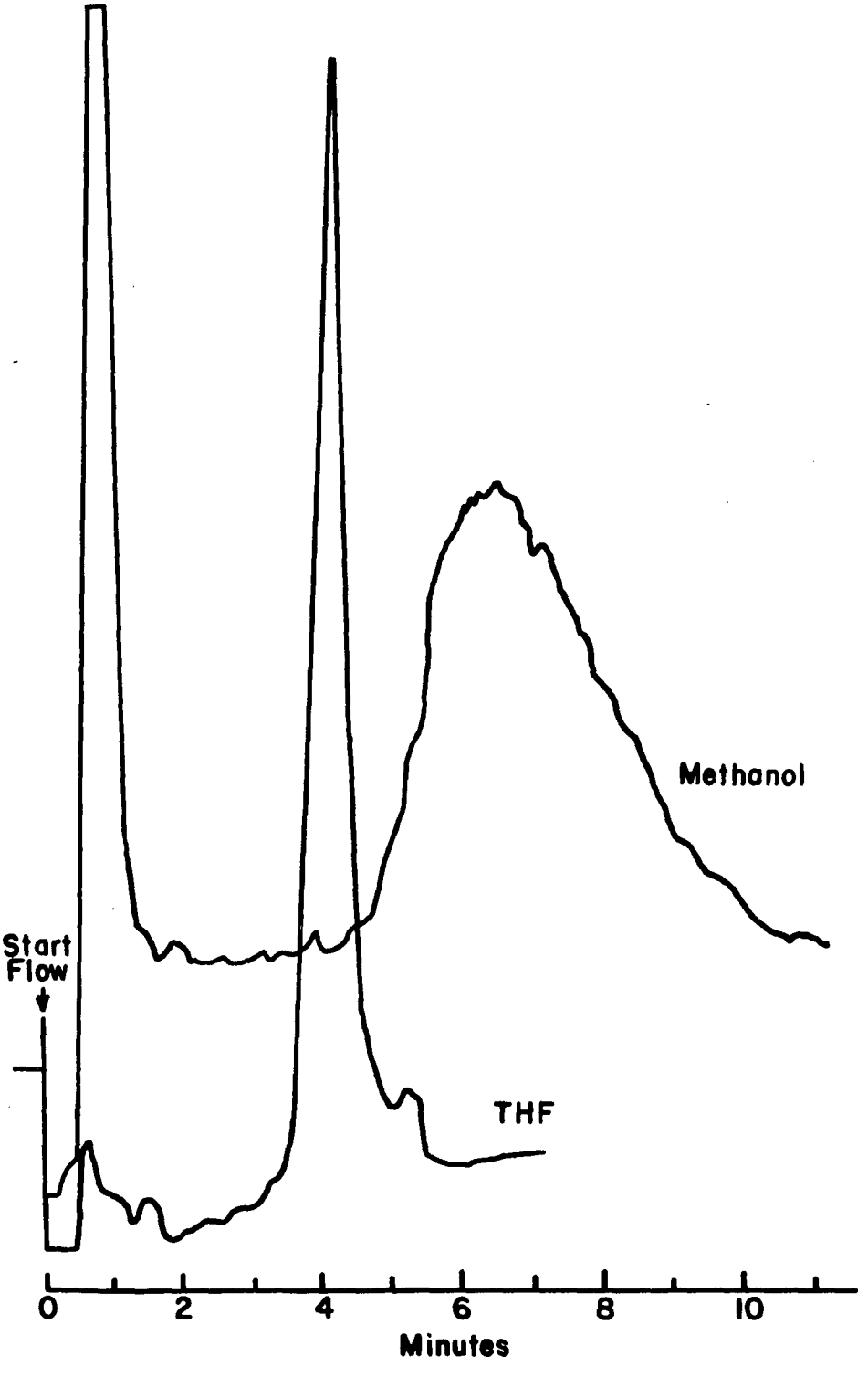

Figure 11. Fractograms of 8μm diameter spheres in 173μm channel in methanol 3.4 ml/min. and THF at 3.2 ml/min.

in the particle's position with respect to the channel wall. Since the particles are moving along very close to the channel surface, it is likely that they will contact the surface, or at least the nearly stagnant solvent near the surface. It is here in this region where surface interactions are important.

Regarding the possible surface effect with THF, (Figures 9, 10 and 11), THF is a rather unusual solvent. It has a planar, hydrocarbon structure which is likely to give it good lubricating properties, yet the oxygen atom is oriented so that it is good hydrogen bond acceptor and will wet or solvate the glass surfaces effectively. Methanol, being more polar and a hydrogen bond donor and accepter, is less able to reduce attractive forces between the glass surfaces. Methanol would also tend to displace THF at the surface even at low methanol concentrations and reduce the lubricating ability of THF. Thus, regarding the higher than expected R values for THF at low flow rates, the difference may be due to a lubricating effect from THF. In general, the magnitude of F_R seems to result primarily from the rotational motion of the particles. However, with a good lubricating and wetting solvent like THF, it is possible that the particles could slide along the channel surface and reduce the effect of the rotational losses of F_R at low flow rates.

CHAPTER 4

SUMMARY AND CONCLUSIONS

Summary

The mechanism of particle retention in steric FFF is much more complex than originally expected. The degree of particle retention is determined not only by particle size, but also by solvent density and viscosity, channel thickness and solvent velocity.

A force model has been presented which is helpful in describing the influence of these factors on particle retention. A graphical method has been suggested for separating and describing the solvent velocity dependent and independent factors affecting particlr retention. A modification of the particle retention equation has been suggested so that the flow-rate dependence of retention is more completely described.

In this equation,

$$R = mV_s + 6\gamma a/h(1 - a/h) \qquad (14)$$

the constant m is a measure of the velocity dependent aspect of particle retention. It accounts for the existence of a hydrodynamic lift force which raises the particles away from the channel wall. The magnitude of this lift force increases with solvent viscosity and density and particle size, and decreases with channel thickness. The second part of this equation, $6\gamma a/h(1 - a/h)$, represents the retention that would

be measured for a particle moving along the channel wall. It is determined by the size of the particle, given by $6a/h(1 - a/h)$, and any factors that would retard the particle relative to the solvent. These factors are reflected in the constant γ, a number less than one. This constant decreases (increases retention) with increasing particle size and solvent viscosity. It appears to be independent of solvent density and channel thickness. There is also some evidence that γ may be affected by surface interactions.

Conclusions

Particle retention in steric FFF has been shown to be dependent, not only on particle size, but also on certain hydrodynamic properties as well. Based on the results of this study, some conclusions can be drawn regarding the use of steric FFF for particle separation and size analysis.

The dependence of retention on factors other than particle size, complicates the use of steric FFF for particle size analysis. Because of the hydrodynamic influences, the particles used for calibration must closely match the sample in density, shape and surface characteristics. Also, the shape of an R versus particle size calibration curve will be flow-rate dependent because of the opposite effects of particle size on retention with respect to the lift force and the retarding force.

However, when used as a separation technique, the dependence of retention on multiple factors increases the selectivity of the technique. Separations can be based on particle density and shape as well as size. This selectivity can be controlled, to a certain extent,

by choosing conditions which enhance or suppress the lift force. The lift force can be increased by increasing flow rate, solvent density or viscosity, or by using thinner channels. These factors can be varied to optimize a separation.

There is still much to be learned about the mechanism of particle retention in steric FFF. Questions remain regarding the effects of particle shape and surface characteristics on retention. Another important aspect to study is the actual particle trajectory through the channel. With the onset of flow, do the particles quickly reach an equilibrium position with respect to the channel wall, or do the particles move away from the wall at a constant or variable rate? These and other questions remain to be answered.

However, since a reasonable understanding of the particle retention has been attained, it would perhaps be more worthwhile to study the practical aspects of steric FFF. Such aspects would include sample capacity, sensitivity, usable size range with respect to channel thickness and also ways to improve efficiency and resolution.

REFERENCES

1. Giddings, J.C.; Fisher, S.R.; Myers, M.N. Am. Lab. 1978, 10, 15.

2. Thompson, G.H.; Myers, M.N.; Giddings, J.C. Anal. Chem. 1969, 41, 1219.

3. Giddings, J.C.; Martin, M.; Myers, M.N. J. Chromatog. 1978, 149, 501.

4. Caldwell, K.D.; Kesner, L.F.; Myers, M.N.; Giddings, J.C. Science, 1972, 176, 296.

5. Giddings, J.C.; Lin, G.C.; Myers, M.N. Separ. Sci., 1976, 11, 553.

6. Giddings, J.C.; Yang, F.J.; Myers, M.N. J. Virol. 1977, 21, 131.

7. Giddings, J.C.; Lin, G.C.; Myers, M.N. J. Liq. Chromatog. 1978, 1, 1.

8. Giddings, J.C.; Yang, F.J.F.; Myers, M.N. Anal. Chem. 1974, 46, 1917.

9. Kirkland, J.J.; Rementer, S.W.; Yau, W.W. Anal. Chem. 1981, 53, 1730.

10. Yau, W.W.; Kirkland, J.J. Anal. Chem. 1984, 56, 1461.

11. Borman, S. Anal. Chem. 1984, 56, 689A.

12. Giddings, J.C.; Myers, M.N. Sep. Sci. and Tech. 1978, 13, 637.

13. Happel, J.; Brenner, H. Low Reynolds Number Hydrodynamics, 1965, Prentice Hall, Inc., Englewood Cliffs, NJ.

14. Giddings, J.C.; Caldwell, K.D.; Nguyen, T.T.; Myer, M.N. Sep. Sci. and Tech. 1979, 14, 935.

15. Rubinow, S.I.; Keller, J.B. J. Fluid Mech. 1961, 11, 447.

16. Segre', G.; Silberberg, A. J. Fluid Mech. 1962, 14, 115.

17. Segre', G.; Silberberg, A. J. Fluid Mech. 1962, 14, 136.